Velocity Condensation for Magnetotactic Bacteria

Jean-François Rupprecht,[1,2] Nicolas Waisbord,[3] Christophe Ybert,[3] Cécile Cottin-Bizonne,[3] and Lydéric Bocquet[1,*]
[1]Ecole Normale Supérieure, Laboratoire de Physique Statistique, UMR CNRS 8550, 24 rue Lhomond, Paris, France
[2]Mechanobiology Institute, National University of Singapore, 5A Engineering Drive 1, 117411, Singapore
[3]Institut Lumière Matière, UMR CNRS 5306, Université Lyon 1, Lyon, France
(Received 26 August 2015; revised manuscript received 3 March 2016; published 20 April 2016)

Magnetotactic swimmers tend to align along magnetic field lines against stochastic reorientations. We show that the swimming strategy, e.g., active Brownian motion versus run-and-tumble dynamics, strongly affects the orientation statistics. The latter can exhibit a velocity condensation whereby the alignment probability density diverges. As a consequence, we find that the swimming strategy affects the nature of the phase transition to collective motion, indicating that Lévy run-and-tumble walks can outperform active Brownian processes as strategies to trigger collective behavior.

DOI: 10.1103/PhysRevLett.116.168101

Bacteria, spermatozoa, or algae have in common the ability to propel themselves in low-Reynolds fluids in order to explore space [1,2]. The directed motion of these swimmers is always affected by stochastic impulses due to noise in the propulsion mechanism. Swimmers undergoing white noise perturbations, which lead to persistent small-amplitude fluctuations of the orientation [3,4], are usually called active Brownian particles (ABPs). In contrast, bacteria like *E. coli* exhibit sudden reorientations of their velocity vector (called tumbles) which are due to stochastic switches in the direction of rotation of propelling flagella [5]. Such dynamics are usually coined as run and tumble (RT). Though ABPs and RTs correspond to two different swimming strategies, in the absence of external torques, their long-time dynamics are similar and lead in both cases to an effective diffusion process [2].

Biological microswimmers can also orient themselves in response to external stimuli, either of chemical or mechanical nature. In particular, the RT walk is essentially thought to provide a mean to move along chemical gradients, called chemotaxis, in which the run duration is modulated with respect to the direction of the stimulus. Other microorganisms have also developed the ability to orient their propelling direction under external mechanical fields, for example under gravity (gravitaxis) or shear or flow gradients (gyro- and rheotaxis) [6–9]. Similar behaviors have been recently reproduced with artificial catalytic swimmers [10–13].

Here we consider the dynamics of swimmers driven under *magnetic* torques, keeping in mind that results generalize to a larger class of mechanical torques. A representative example are magnetotactic bacteria (MB) that behave as self-propelled compasses, due to iron-based organelles orienting the propelling flagella along the magnetic field lines. Since their discovery in 1975, theoretical studies of MB focused on the case of white noise perturbations on the orientation [14,15]. Recent work also demonstrated how superparamagnetic beads could be attached to *E. coli* bacteria, making them reactive to magnetic fields [16].

Here we show that in the presence of an external aligning field, the orientation distribution strongly differs for the two swimming strategies, ABPs and RTs. For RTs, we report a velocity condensation phenomenon that is associated with a divergence of the orientation distribution function in the direction of the field and which occurs above a critical magnetic field. We point out that the resulting behavior is significantly different from a chemotactic response. In the final paragraph, we consider the onset of the collective phase of a swarm with nematic interactions. We show that the nature of the alignment divergence shapes the phase diagram of the isotrope-nematic transition.

The ABPs dynamic is a diffusion process on the direction of the velocity vector $\boldsymbol{V}$, with a fixed speed $|\boldsymbol{V}| = V_0$ [3,4,14]; hence, the dynamics of the alignment angle θ is described by an Ito equation: $d\theta = f(\theta)dt/\tau_B + \sqrt{2dtD_r}\zeta$, where ζ is a Gaussian white noise with $\langle \xi(t)\xi(t')\rangle = \delta_{t,t'}$ and D_r is a rotational diffusion coefficient, and $f(\theta) = -\sin(\theta)$ is the magnetic torque. The magnetic relaxation time τ_B can be expressed as $\tau_B = \xi_0/(mB_a)$, where m is the magnetic moment and ξ_0 is a rotational drag coefficient. The stationary probability distribution for θ corresponds to the Boltzmann statistics

$$P_\infty(\theta) = \mu(\theta)\exp\left[1/(\tau_B D_r)\cos\theta\right]/Z_d, \qquad (1)$$

where Z_d is a dimension dependent normalization factor and $\mu(\theta)$ is the uniform probability measure [$\mu(\theta) = 1/\pi$ in two dimensions or $\sin(\theta)/2$ in three dimensions]. In three dimensions, the mean velocity $V_z = \langle\cos\theta\rangle$ reduces to $V_z = V_0 f[1/(\tau_B D_r)]$, where $f(x) = \coth x - x^{-1}$ is the classical Langevin function [14]. Indeed, Eq. (1) corresponds to the distribution of a passive magnet in a thermal noise [15], with an effective temperature defined as $k_B T_{\text{eff}} = D_r\xi_0$.

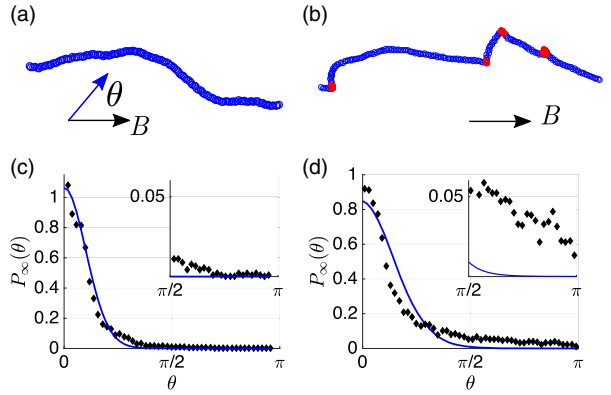

FIG. 1. Trajectories of MB in (a) rich growing medium and (b) poor growing medium environments. (c)–(d) Alignment angle distribution at $B_a = 7 \times 10^{-5}$ T in (c) rich growing medium and (d) poor growing medium environments: (black crosses) experimental histogram and (solid blue line) best ABP fit with (a) $B/D_\perp = 11$ and (b) $B/D_\perp = 4.5$. In (d), there is a 10% discrepancy between the experimental and fitted cumulative distributions (i.e., Kolmogorov-Smirnov norm [20]). (insets) The antiparallel response is enhanced in a poor environment (see Ref. [18]).

From an experimental point of view, MB bacteria usually behave as ABP particles in a standard chemical environment [see Refs. [17,18], and Figs. 1(a) and 1(c)]. However, it has been recently reported that some specific environments can trigger non-Brownian reorientations of MB, as demonstrated on the strains MO-1 [19] and MC-1 [18]. In particular, it has been shown in Ref. [18] that the trajectory of the bacteria presents sudden changes of direction when the concentration in the growing medium is reduced [see Fig. 1(b)]. These kinks are then detected by a tracking algorithm, which shows that the run durations are exponentially distributed (see Ref. [18]). Using the experimental data reported in Ref. [18], we build the experimental histogram presented in Fig. 1(d) from 500 trajectories. The histogram is peaked in the direction of the magnetic field ($\theta = 0$), while maintaining a substantial statistical weight for the antiparallel orientation ($\theta = \pi$). These two features *cannot* be consistently accounted for by an ABP model, which fails to match the statistical weights both in the parallel and in the antiparallel directions of the magnetic field, as highlighted in Fig. 1(d). This inconsistency of the ABP model to reproduce experimental results calls for a shift from the classical Langevin paradigm [14], which can only describe accurately the behavior of magnetotactic bacteria in a medium favorable to growth. As indicated in Ref. [18], this change in the behavior of magnetotactic bacteria in a lesser favorable environment could be related to an evolutionary advantage.

RT walk.—The RT dynamics is composed of runs at a fixed speed V_0 interrupted by instantaneous reorientations. During runs under a magnetic field $\boldsymbol{B_a}$, the evolution of the alignment angle θ (between $\boldsymbol{V}$ and the applied magnetic field $\boldsymbol{B_a}$) is deterministic, with $\dot{\theta} = f(\theta)/\tau_B$. Furthermore, we assume that the duration of each run x (i) is drawn according to a given probability density $\rho(x/\tau_r)$, (ii) is independent of the previous runs, and (iii) is independent of the alignment direction θ (in contrast to chemotaxis). After a tumble, the alignment angle θ_0 is drawn according to the uniform probability measure $\mu(\theta_0)$. We finally define the magnetotactic dimensionless parameter B as

$$B = \tau_r \frac{m|B_a|}{\xi_0}, \tag{2}$$

where τ_r is the mean run time, so that $B = \tau_r/\tau_B$. Remarkably, the estimated values for the magnetotactic number B appear to be of the order unity for MB in typical geomagnetic fields (see Refs. [15,18]).

Angular distribution and velocity condensation.—We seek to obtain the expression for the stationary probability $P_\infty(\theta)$ density for the RT walk, defined so that the probability that the angle θ belongs to the interval $[\theta_1, \theta_2]$ reads $\int_{\theta_1}^{\theta_2} P_\infty(\theta) d\theta$. Partitioning on successive events, we find that $P_\infty(\theta) = \int_0^\infty dt \pi(t) \int_0^\pi d\theta_0 \mu(\theta_0) \delta(\theta - \theta_t(\theta_0))$, where $\pi(t)$ is the distribution of "run" time since the last tumble, and which is to be determined from the distribution of run duration $\rho(x)$ by renewal process theory [21]; θ_0 is the outgoing angle after the tumble, and $\theta_t(\theta_0)$ is the time-dependent evolution operator. For a torque with angular dependence $f(\theta)$, the latter is formally defined as $\theta_t(\theta_0) = F^{(-1)}[F[\theta_0] + Bt]$, with F a primitive of $1/f$ and $F^{(-1)}$ the reciprocal function of F. Using that the function $\theta_0 \to \theta - \theta_t[\theta_0]$ is canceled for $\theta_0 = \theta_0^*(\theta, t) = F^{(-1)}[F[\theta] - Bt]$, one gets

$$P_\infty(\theta) f(\theta) = \int_0^\infty dt \pi(t) (\mu.f)[\theta_0^*(\theta, t)]. \tag{3}$$

Equation (3) holds for an arbitrary torque $f(\theta)$ and spent time distribution $\pi(t)$.

We first consider a magnetic torque $f(\theta) = -\sin(\theta)$ and $\rho(t) = \exp(-t)$ (exponential RT). The spent time distribution is then $\pi(t) = \rho(t)$ [21]. Following the previous definition, we obtain $\theta_0^* = 2 \arctan[\tan(\theta/2) \exp(Bt)]$. In two dimensions, we apply Eq. (3) and we obtain

$$P_\infty(\theta) = \frac{1}{B} \frac{(\tan\theta/2)^{1/B}}{\sin\theta} \int_\theta^\pi d\phi \frac{\mu(\phi)}{(\tan\phi/2)^{1/B}}. \tag{4}$$

A key feature which emerges from Eq. (4) is that the low-θ behavior drastically differs above and below the critical value $B_c = 1$ [see Fig. 2(a)]. For $B < B_c$, $P_\infty(\theta)$ takes a finite value at $\theta = 0$. However, for $B > 1$ we find that

$$P_\infty(\theta) \underset{\theta \to 0}{\sim} \gamma_d^{-1} \theta^{-(1-1/B)}, \tag{5}$$

where $\gamma_2 = 2^{1/B} B \cos[\pi/(2B)]$ in two dimensions and $\gamma_3 = 2^{1/B+1} B^2 \sin[\pi/(2B)]/\pi$ in three dimensions.

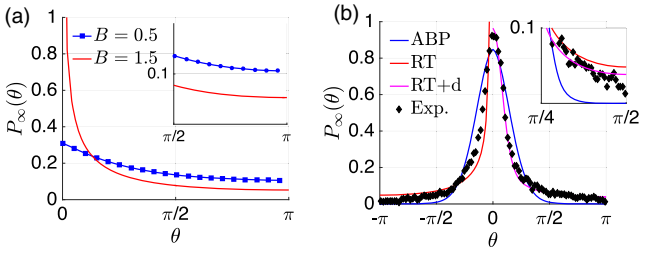

FIG. 2. (a) Probability density $P_\infty(\theta)$ for RTs (2D) for (red solid line) $B = 4$ and (blue circle line) $B = 0.25$. (Inset) The distribution in the opposite direction to the magnetic field remains comparable for both $B = 0.25$ and $B = 4$. (b) Fit of the experiments by the RT model: (black crosses) experimental histogram; (positive side, red solid line) RT fit with $B = 2.3$; (negative side, magenta solid line) RT fit with a mild rotary diffusion with $D_r'/\tau_r = 0.15$ and $B = 3.2$; (both sides, blue solid line) ABP fit with $B/D_\perp = 4.5$. The Kolmogorov-Smirnov error is of 7% for the pure RT model and of 3% for the perturbed RT model.

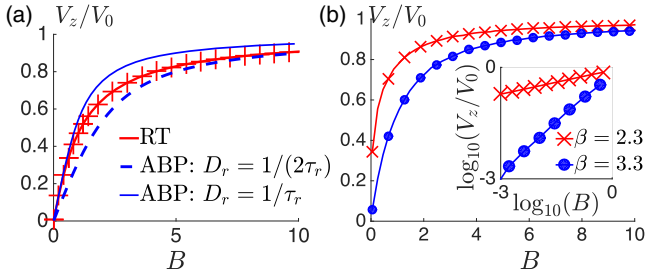

FIG. 3. Forward mean velocity V_z in three dimensions, normalized by the velocity norm V_0: (a) (red line) exact expression for the velocity of a RT with an average step duration τ_r; (blue solid line) ABP with $D_r = 1/\tau_r$; (blue dashed line) ABP with $D_r = 1/(2\tau_r)$. (b) RT Lévy walks case [$\rho(x) \sim x^{-\beta}$, $\beta \leq 3$]: (red crosses) $\beta = 2.30$ and (blue circles) $\beta = 3.30$. Inset: log-scale behavior at $\theta \ll 1$. Inset: in the limit $B \ll 1$, V_z scales as B^ξ (black line), with $\xi = \beta - 2 = 0.30$ for $\beta = 2.30 < 3$ and $\xi = 1$ for $\beta = 3.30 \geq 3$.

At $B = B_c$ a dynamical transition occurs above which the probability density diverges—a property that we call the velocity condensation.

Extension and robustness.—We first remark that the condensation phenomenon is maintained for alternative aligning torques, provided the torque is strong enough around $\theta = 0$. Consider that $f(\theta) \sim -\theta^n$ for $\theta \ll 0$, then (i) if $n > 1$ and for exponential RT, the torque term is too weak for the velocity condensation to occur, and (ii) if $n < 1$, the condensation always occurs, as the $\theta = 0$ state can be attained after a finite run time. Second, the strict mathematical divergence disappears in the presence of a rotary Brownian noise on the velocity orientation during runs, characterized by a diffusion coefficient D_r'. As $\theta \to 0$, the diffusive noise eventually dominates over the vanishing torque and the orientation probability scales as $P_\infty(\theta) \propto \exp[-\theta^2 B\tau_r/(2D_r')]$ in the region $\theta \in [0, D_r'/(\tau_r B)]$). However, provided that the rotary diffusion coefficient noise is relatively small ($D_r'/\tau_r < 1$), the probability density of RTs is sharply peaked when $B > 1$.

RT fit of experiments.—We now compare the prediction of the RT model to the experimental histogram presented in Fig. 2(b). In contrast to the ABP model fit, which cannot account for the sharp peak in the orientation distribution without underestimating it in the antiparallel directions, the RT walk provides the appropriate statistical weight to both the parallel and the antiparallel directions. The increase in the quality of the fit can be measured through the Kolmogorov-Smirnov norm [20], which quantifies the discrepancy between the cumulative distributions. The quality of the fit is increased by considering a RT walk in which runs are perturbed by a mild rotary noise ($D_r'/\tau_r = 0.15$). We conclude that, in spite of this small rotary diffusion that affects the orientation of bacteria, the distribution in Fig. 2 is still very sharply peaked in the direction of the magnetic field.

We conclude that the RT walk is more efficient than the ABP process to sample both the parallel and antiparallel directions to the magnetic field. Our intuitive explanation is that, in contrast to a diffusion process, all orientations are sampled after a tumble, and, in particular, the antiparallel directions to the magnetic field.

Mean velocity and diffusion.—From the orientation distribution, we can calculate the mean velocity of the RTs. The averaged velocity in the direction of the magnetic field is defined as $V_z = V_0\langle\cos\theta\rangle$. Using the previous expressions for the distribution function, one gets

$$V_z = V_0 \frac{1}{B}\int_0^1 dw w^{1/B-1} g_d(w). \tag{6}$$

In two dimensions, $g_2(w) = (1-w)/(1+w)$ and $V_z/V_0 = \{\psi^{(0)}(B + 1/2B) - \psi^{(0)}(1/2B)\}/B - 1$, with $\psi^0(z) = \Gamma'(z)/\Gamma(z)$ and $\Gamma(z)$ is the Gamma function [22]. In three dimensions, $g_3(w) = (1 - w^4 + 4w^2\log(w))/(w^2-1)^2$ and Eq. (6) reads $V_z/V_0 = \psi^{(1)}[1/(2B)]/(2B^2) - 1/B - 1$, where $\psi^1(z)$ stands for the derivative of $\psi^0(z)$ [22]. This result is plotted in Fig. 2 against the results obtained for ABP in terms of the Langevin equation. Interestingly, there is no strong signature of the onset of the velocity condensation on the mean velocity. Furthermore, while the expression for V_z differs from the Langevin prediction for ABPs, we observe that for a general B, the curve of the RT velocity lies in between those for ABPs with $D_r = 1/(2\tau_r)$ and $D_r = 1/(\tau_r)$ [see Fig. 3(a)]. We obtain similar conclusions concerning the diffusion coefficient $D_\perp$ in the transverse direction (xOy) (see Ref. [23]), suggesting that, in spite of the velocity condensation, RTs are as efficient as ABPs in exploring their environment.

Chemotaxis.—Chemotaxis refers to an angular dependence in the mean duration of a run [5]. We first consider the

parallel chemotaxis case $\tau_r(\theta) = 1 + \chi\cos(\theta)$, which favors runs in the direction of the magnetic field when $\chi > 0$. In units of τ_r, the Fokker-Planck equation reads [27]

$$B\partial_\theta(\sin\theta P) - (1 + \chi\sin\theta)P(\theta) = -(1 + \chi\langle P\sin\theta\rangle),$$

where $\langle P|\sin\theta\rangle = \int_{-\pi}^{\pi} duP(\phi)\sin(\phi)$. We show that the solution reads

$$P(\theta) = \gamma\frac{\tan(\theta/2)^{1/B}}{\sin(\theta)^{1-(\chi/B)}}\int_\theta^\pi d\phi\frac{\sin(\phi)^{-\chi/B}}{\tan(\phi/2)^{1/B}}, \qquad (7)$$

for $\theta > 0$, where $\gamma = 1 + \chi\langle p|\sin\theta\rangle$. The constant $\langle p|\sin\theta\rangle$ is found as a solution of the self-consistency equation: $\langle p|\sin\theta\rangle = \langle f_p|c\rangle/(\lambda_0 - \epsilon\langle f_p|c\rangle)$. From Eq. (7), we find that a positive parallel chemotaxis lowers the value of the critical magnetotatic constant above which the velocity condensation occurs, as $B_c = 1 - \chi$. In contrast, a transverse chemotactic field, as defined by $\tau_r(\theta) = 1 + \chi\sin(\theta)$, will not change the value $B_c = 1$ (see the Supplemental Material [23]).

Lévy walks.—We show that the velocity condensation phenomenon is further amplified for systems exhibiting a Lévy statistics of the run period. Lévy walks are characterized by heavy-tailed distribution of run duration: $\rho(x) = \mathbb{1}_{x>1}(\beta - 1)/x^\beta$ with $2 < \beta < 3$. The value $\beta = 2$ corresponds to a predicted optimal search strategy [28]. To apply Eq. (3), we notice that $\pi(t) = (\beta - 2)/(\beta - 1)t^{1-\beta}$, when $t > 1$ [21], and that the function $t \to \sin(\theta_0^\star)$ is sharply peaked around $t^* = -\log[\tan(\theta/2)]/B$. We find that the velocity condensation occurs for any $\beta > 2$ as

$$P_\infty(\theta) \underset{\theta\to 0}{\sim} \gamma\frac{B^{\beta-1}(\beta - 2)}{(\beta - 1)}\frac{1}{\theta[\log(1/\theta)]^{\beta-1}}, \qquad (8)$$

where $\gamma = 0.46\ldots$ both in two and three dimensions. This expression corresponds to an enhanced condensation compared to exponentially distributed runs. The mean velocity is found in terms of an expression analogous to Eq. (6). We truncate the functions $g_d(w)$ to its first order expansion at $w = 1$ to obtain,

$$V_z/V_0 \underset{B\to 0}{\sim} \gamma_d\frac{\Gamma(3 - \beta)}{\beta - 1}B^{\beta-2}, \qquad (9)$$

where $\gamma_2 = 1/2$ and $\gamma_3 = 2/3$. The nonanalytical scaling $B^{\beta-2}$ in Eq. (9) corresponds to a highly sensitive directional response at the onset of the stimulus detection (from $B = 0$ to $B > 0$). In comparison, the velocity V_z is proportional to B when $B \ll 1$ for ABPs as well as for RTs with a finite second moment for the run duration [e.g., $\beta \geq 3$ in Fig. 3(b)].

Collective behavior.—We finally consider the consequence of the velocity condensation on the collective behavior of a swarm [29–36]. We adapt the Maier-Saupe mean-field treatment for a highly concentrated swarm of interacting self-propelled rods [29] (see also Refs. [30–32]). In contrast to previous results, which assumed a Boltzmann distribution for the orientation distribution Eq. (1), we use here the precise statistic of the orientation from Eq. (3). Following Refs. [29,32], we consider that interactions between bacteria result in an effective torque acting uniformly on each bacterium: $f(\theta) = -U_0A[P_\infty]\sin(2\theta)$, where U_0 is the interaction strength and A measures the local nematic order and is defined as $A[P_\infty] = \int_0^\pi du\cos(2u)P_\infty(u)$ in two dimensions and $A[P_\infty] = \int_0^\pi du(3\cos^2 u - 1)P_\infty(u)$ in three dimensions. Using Eq. (3), we compute the probability distribution $P_\infty(S)$ that corresponds to an imposed value $S = A[P_\infty]$. The order parameter, denoted $S^\star$, is then found as the solution of the following self-consistency equation: $S^\star = A[P_\infty(S^\star)]$. For RTs with exponential runs, the isotropic phase ($S^\star = 0$) is destabilized above a critical value of the interaction strength $U_0^{(c)} > 1.87.\tau_r^{-1}$ in favor of the nematic phase. The phase diagram is alike for ABP swimmers [32]. However, the probability distribution diverges in both directions $\theta = 0$ and $\theta = \pi$ for RTs within the nematic phase (three dimensions). Within Onsager's theory, the quantity $1/U_0^{(c)}$ can be interpreted as an excluded volume induced by steric interactions [37].

For RT Lévy walks, the phase diagram is drastically changed due to destabilization of the isotrope phase (see Fig. 4). Indeed, the order parameter should satisfy by the following self-consistency equation:

$$S^\star = \gamma_d\frac{\Gamma(3 - \beta)}{\beta - 1}(U_0S^\star)^{\beta-2}, \qquad S^\star \ll 1, \qquad (10)$$

where $\gamma_3 = (2^\beta - 4)/5$ in three dimensions. Because of the behavior of the probability distribution in Eq. (10), Eq. (9) displays an nonanalytical behavior with $S^\star \ll 1$. This $S^{\beta-2}$ behavior implies that a solution $S^\star > 0$ necessarily exists for any value of the interaction strength $U_0 > 0$. Hence, we find that the isotropic phase is intrinsically unstable, as $U_0^{(c)} = 0$, which corresponds to a diverging excluded

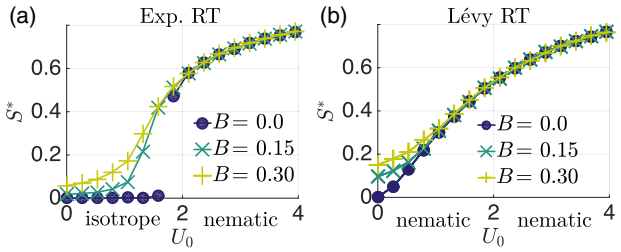

FIG. 4. Phase diagrams of the order parameter S^* in three dimensions in terms of the interaction strength U_0, and for several values of B [see Eq. (2)]: (a) RTs with exponentially distributed runs, (b) Lévy walks with $\beta = 2.6$: $S^* > 0$ for $U_0 > 0$ even at $B = 0$ (blue circle curve); hence, the isotropic phase is intrinsically unstable.

volume. Similar conclusions can be drawn in two dimensions [$\gamma_2 = 1/2$ in Eq. (10)].

Experimentally, it appears that bacteria [38,39] and immune cells [40] can perform Lévy walks with an exponent $\beta < 3$, which is within our predicted regime of a high sensitivity at the onset of the stimulus detection and to collective motion [see Eqs. (9) and (10)].

Conclusion.— In this Letter, we exhibit a divergence in the orientation response of the RT walk under torque. This divergence is required to account the high directional response of tumbling magnetotactic swimmer, even when perturbed by a Brownian rotary noise [see Fig. 2(b)]. Experiments on MC–1 bacteria confirm the observation that tumbling bacteria exhibit a stronger parallel or antiparallel response to the magnetic field, which cannot be described by the standard ABP model. Based on our analytical expressions for the orientation distribution, we find that the noise statistic has a crucial impact on the onset of collective motion. The fact that for Lévy runs, the transition occurs in the limit of an infinite excluded volume hints at a possible extension of Onsager's theory [37] in terms of a dynamical excluded volume that depends on the noise statistic.

We thank J. Prost for suggesting the idea of a dynamical excluded volume. We also thank François Detcheverry for fruitful discussions. N. W. was supported by the AXA fund.

*lyderic.bocquet@ens.fr

[1] E. M. Purcell, Am. J. Phys. **45**, 3 (1977).
[2] M. E. Cates, Rep. Prog. Phys. **75**, 042601 (2012).
[3] B. ten Hagen, S. van Teeffelen, and H. Löwen, J. Phys. Condens. Matter **23**, 194119 (2011).
[4] P. Romanczuk, M. Bär, W. Ebeling, B. Lindner, and L. Schimansky-Geier, Eur. Phys. J. Spec. Top. **202**, 1 (2012).
[5] H. C. Berg and R. M. Berry, Phys. Today **58**, 64 (2005).
[6] W. M. Durham, E. Climent, and R. Stocker, Phys. Rev. Lett. **106**, 238102 (2011).
[7] D.-P. Häder, R. Hemmersbach, and M. Lebert, *Gravity and the Behavior of Unicellular Organisms* (Cambridge University Press, Cambridge, England, 2005), p. 258.
[8] K. Fukui and H. Asai, Biophys. J. **47**, 479 (1985).
[9] X. Garcia, S. Rafaï, and P. Peyla, Phys. Rev. Lett. **110**, 138106 (2013).
[10] J. Palacci, S. Sacanna, A. Abramian, J. Barral, K. Hanson, A. Y. Grosberg, D. J. Pine, and P. M. Chaikin, Sci. Adv. **1**, e1400214 (2015).
[11] B. Hagen, F. Ku, R. Wittkowski, D. Takagi, H. Lo, and C. Bechinger, Nat. Commun. **5**, 4829 (2014).
[12] A. Zöttl and H. Stark, Phys. Rev. Lett. **108**, 218104 (2012).
[13] W. Gao, D. Kagan, O. S. Pak, C. Clawson, S. Campuzano, E. Chuluun-Erdene, E. Shipton, E. E. Fullerton, L. Zhang, E. Lauga, and J. Wang, Small, **8**, 460 (2012).
[14] R. P. Blakemore, Annu. Rev. Microbiol. **36**, 217 (1982).
[15] R. Nadkarni, S. Barkley, and C. Fradin, PLoS One **8**, e82064 (2013).
[16] M. M. van Oene, L. E. Dickinson, F. Pedaci, M. Köber, D. Dulin, J. Lipfert, and N. H. Dekker, Phys. Rev. Lett. **114**, 218301 (2015).
[17] R. B. Frankel, R. P. Blakemore, and R. S. Wolfe, Science **203**, 1355 (1979).
[18] N. Waisbord, C. Lefvre, L. Bocquet, C. Ybert, and C. Cottin-Bizonne, arXiv:1603.00490.
[19] S. D. Zhang, N. Petersen, W. J. Zhang, S. Cargou, J. Ruan, D. Murat, C. L. Santini, T. Song, T. Kato, P. Notareschi, Y. Li, K. Namba, A. M. Gué, and L. F. Wu, Environ. Microbiol. Rep. **6**, 14 (2014).
[20] F. J. Massey, J. Am. Stat. Assoc. **46**, 68 (1951).
[21] W. Feller, *An Introduction to Probability Theory and Its Applications* (Wiley, New York, 1968), Vol. 2, p. 509.
[22] I. M. Ryzhik and I. S. Gradstein, *Tables of Series, Products, and Integrals* (Academic Press, 1957), p. 438.
[23] See Supplemental Material at http://link.aps.org/supplemental/10.1103/PhysRevLett.116.168101 for several additional proofs and approximate analytical expressions for the orientation distribution, which includes Refs. [24–26].
[24] M. Schienbein and H. Gruler, Bull. Math. Biol. **55**, 585 (1993).
[25] C. W. Gardiner, *Handbook of Stochastic Methods for Physics, Chemistry and Natural Sciences* (Springer, New York, 2004).
[26] R. Balagam and O. A. Igoshin, PLoS Comput. Biol. **11**, e1004474 (2015).
[27] R. N. Bearon and T. J. Pedley, Bull. Math. Biol. **62**, 775 (2000).
[28] G. M. Viswanathan, S. V. Buldyrev, S. Havlin, M. G. E. da Luz, E. P. Raposo, and H. E. Stanley, Nature (London) **401**, 911 (1999).
[29] M. Doi and S. F. Edwards, *The Theory of Polymer Dynamics* (Clarendon Press, Oxford, 1988).
[30] F. Bolley, J. A. Cañizo, and J. A. Carrillo, Appl. Math. Lett. **25**, 339 (2012).
[31] P. Degond, A. Frouvelle, and J.-G. Liu, J. Nonlinear Sci. **23**, 427 (2013).
[32] B. Ezhilan, M. J. Shelley, and D. Saintillan, Phys. Fluids **25**, 070607 (2013).
[33] E. Bertin, A. Baskaran, H. Chaté, and M. C. Marchetti, Phys. Rev. E **92**, 042141 (2015).
[34] F. Peruani, J. Starruß, V. Jakovljevic, L. Søgaard-Andersen, A. Deutsch, and M. Bär, Phys. Rev. Lett. **108**, 098102 (2012).
[35] A. Baskaran and M. C. Marchetti, Phys. Rev. E **77**, 031311 (2008).
[36] A. Baskaran and M. C. Marchetti, Phys. Rev. Lett. **101**, 268101 (2008).
[37] L. Onsager, Ann. N.Y. Acad. Sci. **51**, 627 (1949).
[38] E. Korobkova, T. Emonet, J. M. G. Vilar, T. S. Shimizu, and P. Cluzel, Nature (London) **428**, 574 (2004).
[39] G. Ariel, A. Rabani, S. Benisty, J. D. Partridge, R. M. Harshey, and A. Be'er, Nat. Commun. **6**, 8396 (2015).
[40] T. H. Harris, E. J. Banigan, D. A. Christian, C. Konradt, E. D. Tait Wojno, K. Norose, E. H. Wilson, B. John, W. Weninger, A. D. Luster, A. J. Liu, and C. A. Hunter, Nature **486**, 545 (2012).